Future droughts in northern Italy: high-resolution projections using EURO-CORDEX and MED-CORDEX ensembles

Alice Baronetti, Vincent Dubreuil, Antonello Provenzale, Simona Fratianni

Climatic Change (2022) 172: 22
https://doi.org/10.1007/s10584-022-03370-7

Future droughts in northern Italy: high-resolution projections using EURO-CORDEX and MED-CORDEX ensembles

Alice Baronetti[1,3] · **Vincent Dubreuil**[2] · **Antonello Provenzale**[3] · **Simona Fratianni**[1]

Received: 23 November 2021 / Accepted: 8 May 2022 / Published online: 1 June 2022

Abstract
We analyse the expected characteristics of drought events in northern Italy for baseline (1971–2000), near (2021–2050), and far (2071–2100) future conditions, estimating the drought spatial extent and duration, the percentage of affected area, and the frequency of drought episodes. To this end, daily ensembles of precipitation and temperature records from Global Climate Models (GCMs) and Regional Climate Models (RCMs) pairs, extracted from EURO-CORDEX and MED-CORDEX for the RCP 4.5 and 8.5 scenarios, are collected at spatial resolution of 0.11 degrees. Before the analysis, model outputs are validated on daily weather station time series, and scaling factors for possible use in bias correction are identified. Annual temperature and precipitation anomalies for near and far future conditions are investigated; drought events are identified by the standardized precipitation evapotranspiration index and standardized precipitation index at the 12-, 24-, and 36-month timescales. This study highlights the importance of using multiple drought indicators in the detection of drought events, since the comparison reveals that evapotranspiration anomaly is the main triggering factor. For both scenarios, the results indicate an intensification of droughts in northern Italy for the period 2071–2100, with the Alpine chain being especially affected by an increase of drought severity. A North-to-South spatial gradient of drought duration is also observed.

Keywords CORDEX project · Future projections · Drought · Anomalies · Bias correction · Drought indices

✉ Alice Baronetti
alice.baronetti@igg.cnr.it

[1] Earth Sciences Department, University of Turin, Turin, Italy

[2] Université Rennes 2, UMR 6554, CNRS, LETG, Rennes, France

[3] Institute of Geosciences and Earth Resources, National Research Council, Pisa, Italy

1 Introduction

Droughts are natural hazards modulated by climate variability, and they occur on a variety of different spatial and temporal scales (Mishra and Singh, 2010). In contrast to aridity, that is a permanent climatic feature, droughts are generated by a temporary imbalance of water availability. Determining the spatial and temporal distribution of droughts is not immediate, as droughts develop slowly and are characterised by uncertain severity, duration, and frequency (Dubreuil, 1997; Vicente-Serrano et al. 2010). Cascade effects such as intensification of wildfires are also to be expected (Turco et al. 2018). The Mediterranean region is affected by strong drought episodes, owing also to the high interannual variability of precipitation that reduces freshwater stores (Drumond et al. 2017). Drought episodes during the wet season have significant impact on agriculture and economy, requiring massive use of surface and groundwater (Lamy and Dubreuil, 2013).

Prolonged Mediterranean and European droughts, associated to severe impacts, became more frequent since the 1970s. Manzano et al. (2019) found a strong link between the spatial and temporal distribution of droughts and the changes in atmospheric circulation patterns. The remarkable drought event recorded in summer 2003 affected most central and western Europe and it was characterised by persistent anticyclonic conditions, generated by a strong positive phase of the East Atlantic teleconnection pattern (Luterbacher et al. 2004). Another important factor in the insurgence of summer droughts is the presence of a dry soil moisture anomaly at the end of spring, associated for example with low winter precipitation (D'Andrea et al. 2006). An important drought event was recorded in 2011, mainly affecting south-western Europe, leading to a severe soil moisture deficit in northern Italy, in southern France and in the Iberian Peninsula (Spinoni et al. 2015). This event was characterised by a precipitation deficit that started in winter 2011, generated by the negative phase of the Western Mediterranean Oscillation circulation pattern. During summer 2017, most of southern and western Europe suffered from a major drought episode. The whole event was characterised by weakened zonal circulation and intensification of high-pressure systems. In Spain and Italy, crops were severely affected, with a resulting reduction in agricultural production (García-Herrera et al. 2019). In northern Italy, drought episodes have generally increased since 1983, with a longer duration of the lean period of the main Italian river, the Po (Baronetti et al. 2020).

Future climate projections can be obtained using the Representative Concentration Pathways (RCPs) for the global climate model (GCM) simulations developed in the framework of the Coupled Model Intercomparison Project Phase 5 (CMIP5, Taylor et al. 2012), with typical spatial resolution in the range 100–250 km. To represent climate variability on smaller scales, Regional Climate Models (RCMs) are nested into global models to provide a dynamical downscaling of the GCMs, with a spatial resolution in the range 10–50 km (Colmet-Daage et al. 2018). The CORDEX project, in particular, has provided high spatial resolution models for different European regions. The two sub-projects Euro-CORDEX (Jacob et al. 2014) and Med-CORDEX (Ruti et al. 2015) have produced present-day and future simulations at 12 km. A detailed analysis of future projections for the Mediterranean basin is provided by Spinoni et al (2018), who analysed a large number of simulations based on a combination of GCMs and RCMs. Their analysis highlighted a significant climatic change for the Mediterranean basin. The marked negative precipitation trend, linked with a significant temperature increase, could presumably lead to more severe drought episodes. For Italy, Desiato et al. (2015) have collected four RCMs models with spatial resolution of 50 km, belonging to the Med-CORDEX subproject. The authors

found a temperature increase of 2.5 °C for RCP 4.5 and of 4.4 °C for RCP 8.5 in the period 2061–2090, compared to the reference period 1971–2010. Spatial distribution maps show that northern Italy, in particular the western sector, is most sensitive to such temperature increase, see e.g. Brussolo et al. (2022). For precipitation, a slight decrease of about 1.5% with respect to the reference period is expected for most of Italy by the end of the century. In the Alpine area, by contrast, weak positive precipitation anomalies are foreseen.

In past years, several studies have been devoted in the investigation of future precipitation and temperature changes in a continental-scale context, such as the whole Mediterranean Basin (Lopez-Bustins et al. 2013) or the whole of Europe (Teuling, 2018s). Future droughts and water scarcity were investigated for the European Alps, using RCM and GCM simulations (e.g. Terzi et al. 2021; Brunner et al. 2019). Owing to the significant precipitation decrease, future drought events for southern Italy were explored (Critto et al. 2016). On the contrary, fewer efforts were devoted to the study of past and future droughts in northern Italy, a borderline Mediterranean climate region. This area is historically rich in water resources and the availability of water for irrigated and rainfed farming is traditionally high. However, drought events have increased in the last twenty years, and such dry and warm conditions determine the prolongation of the Po River lean period. The present work addresses, for the first time, the high-resolution analysis of baseline (1971–2000), near (2021–2050), and far future (2071–2100) drought episodes for northern Italy, providing spatial maps of the estimated drought distribution. The study is performed at weekly scale by analysing GCMs-RCMs pairs belonging to the EURO-CORDEX and MED-CORDEX sub-projects at 12 km resolution, considering both the historical runs and the future simulations nested into the RCP 4.5 and RCP 8.5 GCM scenarios. First, a regional model validation on ground data is performed, using an innovative application of two softwares (Co.Temp and Co.Rain). Model biasses are determined and the most reliable model configurations for northern Italy are identified and then used in the subsequent analysis. Near future and far future annual anomalies for precipitation and temperature are investigated and the *SPEI* and *SPI* drought indices at 12-, 24-, and 36-month timescales are used in the drought analysis. The expected frequency of drought events and their magnitude and the percentage of area affected for specific severity thresholds and the temporal trends are quantified. The spatial extent of baseline and future drought episodes and the possible mechanisms and triggering factors are finally discussed.

2 Study area

Northern Italy includes the Po Plain, surrounded by two mountain chains, the Alps at the northern and north-western boundaries and the Apennines at the southern boundary (Fig. 1). The northern Adriatic Sea constitutes the eastern boundary. The Po Plain represents the main Italian plain and it covers 46,000 km^2, 71% of all the Italian plains. It is crossed by the 652-km long river Po, the largest Italian river. The Po River flows eastward to the Adriatic Sea and it is fed by the water of all the tributaries streaming from the Apennines and the Alps. The orogenesis of the Alps and Apennines influenced the evolution of northern Italy, resulting in a complex topographical structure. The highest peaks are in the Alps, having mean elevation of 2500 m asl and maximum altitude at the Mont Blanc (4810 m asl). In the Apennines, the highest peak is Monte Cimone, with altitude 2165 m asl. This orographic configuration promotes the formation of a positive atmospheric pressure difference (4–8 hPa) between the upwind and the downwind sides of the Alps, with foehn airflows coming from North, North-West,

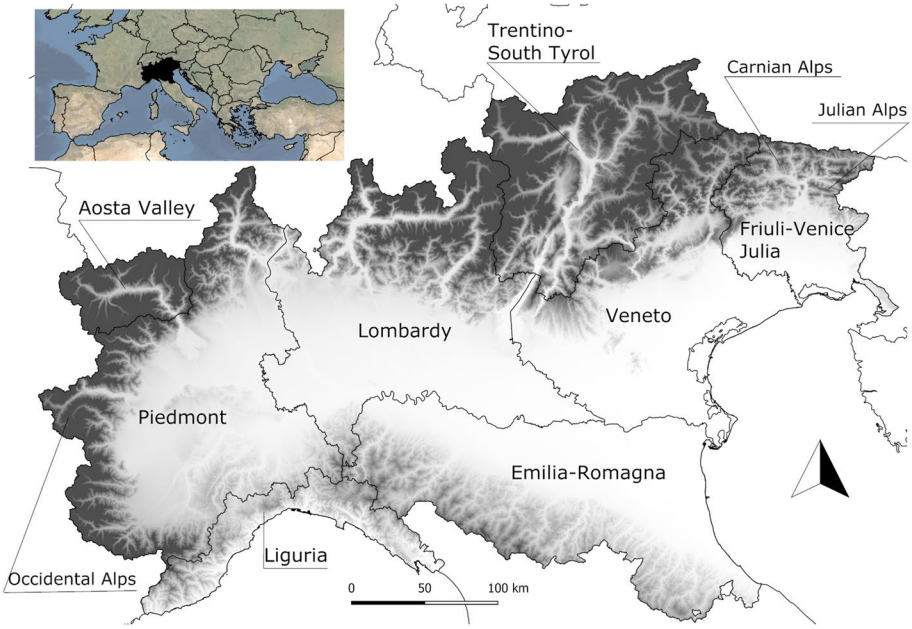

Fig. 1 Map of the study area (northern Italy)

and West especially during February, March, and April (Fratianni et al. 2009). Northern Italy hydrology has an important contribution from glacier melt and the total runoff from glacierized surfaces is expected to significantly increase in the next 30 years and subsequently to decrease at the end of the twenty-first century (Farinotti et al. 2016).

As indicated in the Koppen classification, the most frequent climate observed in northern Italy is hot summer temperate (Cfa), especially in the Po Plain (Fratianni and Acquaotta, 2017; Vallorani et al. 2018). At the foothills, climate is temperate oceanic (Cfb) and the presence of several lakes has a mitigating influence, allowing the cultivation of Mediterranean crops (wine, olives, citrus fruits). Along the mountain ranges a cold temperate climate (Dw) is present, and the mean temperature of the coldest month is > -3 °C (Nigrelli et al. 2018). In northern Italy, winters are relatively dry and cold, and the mean temperature recorded in the Po Valley during the reference period 1971–2010 is between 1 and 4 °C. July temperatures range between 22 and 24 °C in the Po Valley (Bigi et al. 2012) and strong summer thunderstorms are common near the Alps. The foothill (Prealpine) zone is the rainiest sector, with annual precipitation of 1500–2000 mm, and in the Po Valley, the annual precipitation ranges between 600 and 800 mm. The highest rainfall amounts are reached in spring and autumn, while the lowest precipitation is observed in winter and summer. Snow episodes are common during the period from early December to early March (Fratianni and Acquaotta, 2017).

3 Data set

RCMs simulations exhibit uncertainties that are especially marked in areas with complex topography. For this reason, it is recommended to analyse an ensemble of simulations (Teutschbein and Seibert, 2012). In the following, the RCM outputs of the two sub-projects

EURO-CORDEX (https://www.euro-cordex.net/) and MED-CORDEX (https://www.medcordex.eu/) were collected and processed. Here, we considered 18 daily maximum and minimum temperature and 18 daily precipitation ensembles at spatial resolution of 0.11 degree (Table 1) from the RCMs RACMO22E, HIRHAM5, CCLM4, and ALADIN52, driven by the EC-EARTH, MPI-ESM, HadGEM2, and CM5 GMCs. Here, we considered the historical runs and the outputs for the two representative concentration pathways RCP 4.5 and RCP 8.5. The RCP 8.5 scenario is characterised by very high greenhouse gas emissions and global temperature is expected to increase between 2.6 and 4.8 °C by the end of the century. The RCP 4.5 scenario is intermediate, with global temperature increase between 1.4 and 3.1 °C (IPCC, 2022). From the selected ensembles, we extracted the northern Italian area using the following vertices, expressed in WGS84 coordinates: 47.667 North, 43.242 South, 14.566 East, and 6.032West.

3.1 Model validation and scaling factor estimate

We first considered a model validation procedure to detect which GCMs/RCMs pairs perform best in northern Italy. For this purpose, 10 daily precipitation and temperature series (reference series) were extracted from the GCMs/RCMs historical runs (1971–2000 period) and compared to the corresponding 30-year-long quality controlled and homogenised data series recorded at the ground (candidate series), obtained from the database produced by Baronetti et al. (2020) for northern Italy. The statistical comparison between reference and candidate series was performed with the innovative use of Co.Temp (Guenzi et al. 2019) for temperature and Co.Rain (Guenzi et al. 2017) software algorithms for precipitation. These algorithms were developed to detect discontinuities in precipitation and temperature series due to changes in measurement devices. Such methods compare a temperature (or precipitation) signal coming from an old instrument (taken as candidate) with that recorded by a more recent device (taken as reference), with at least 5 years of overlapping. The statistical approach includes the Root Mean Square Error (*RMSE*) to show differences or similarities between the series. This allows to estimate whether the two signals recorded (statistically) similar temperature (or precipitation) weak, mean, heavy, and extreme events. After that, the two algorithms estimate the number of candidate and reference events included in these ranges. Using the more reliable model pairs, we estimated the northern Italy bias scaling factor for precipitation and temperature, in case one wants to scale the RCM raw mean values using a linear scaling bias correction method (Shrestha et al. 2017). For this purpose, the precipitation scaling factor P_{Sf} is estimated as:

$$P_{Sf} = \frac{P_{\text{mean\_obs}}}{P_{\text{mean\_raw}}} \tag{1}$$

Table1 GCM-RCM model pairs selected from the EURO-CORDEX and MED-CORDEX sub-projects. The models that provided the less reliable results for northern Italy during the validation phase are shaded in grey

N°	*Historical*	*N°*	*RCP4.5*	*N°*	*RCP8.5*
1	EC-EARTH-RACMO22	**7**	EC-EARTH-RACMO22	**13**	EC-EARTH-RACMO22
2	EC-EARTH-HIRHAM5	**8**	EC-EARTH-HIRHAM5	**14**	EC-EARTH-HIRHAM5
3	MPI-ESM-CCLM4	**9**	MPI-ESM-CCLM4	**15**	MPI-ESM-CCLM4
4	HadGEM2-CCLM4	**10**	HadGEM2-CCLM4	**16**	HadGEM2-CCLM4
5	HadGEM2-RACMO22	**11**	HadGEM2-RACMO22	**17**	HadGEM2-RACMO22
6	CM5-ALADIN52	12	CM5-ALADIN52	**18**	CM5-ALADIN52

where $P_{\text{mean\_obs}}$ is the mean annual value of observed precipitation at the ground and $P_{\text{mean\_raw}}$ is the mean annual value of raw precipitation estimated from the historical runs of the GCM/RCM model pairs (Ghimire et al. 2019).

The temperature scaling factor T_{Sf} is given by:

$$T_{Sf} = T_{\text{mean\_obs}} - T_{\text{mean\_raw}} \tag{2}$$

where $T_{\text{mean\_obs}}$ is the mean annual value of observed temperature at the ground and $T_{\text{mean\_raw}}$ is the mean annual value of raw temperature estimated from the historical runs of the GCM/RCM model pairs (Fang et al. 2015).

We also tested the significance of annual precipitation and temperature scaling factors for northern Italy. First, the ratio between the standard deviation (σ) of ground data and that of GCM/RCM simulations for the 1971–2000 period was considered. Afterwards, the ratio between the annual scaling factor and the model standard deviation for the baseline was obtained for each model pair. Note, however, that in the following drought analysis we do not use bias corrections as we compare the model (near or far) future with the model baseline.

4 Methods

To detect the main baseline (1971–2000), near (2021–2050), and far (2071–2100) future weekly drought episodes, the daily precipitation and temperature series of the best-performing models were averaged at weekly temporal scale. The estimate of drought indices requires homogenous periods; thus, it was not possible to use calendar weeks as reference periods because the first day of each year can fall on a different week day. To avoid the occurrence of lap years, each month was divided into 4 weekly periods: the first week goes from the 1st to the 8th day; the second from the 9th to the 15th day; the third from the 16th to the 22nd day; and the fourth week from the 23rd until the end of the month (Vicente-Serrano et al. 2017).

Before the drought analysis, for each GCM/RCM pair, near and far future precipitation and temperature anomalies were investigated. For both concentration pathways, the mean annual maximum and minimum temperature anomalies were calculated as the difference between the mean annual average in the near (2021–2050) or far (2071–2100) future and the mean annual average of the baseline (1971–2000, Toreti and Desiato, 2008). The same approach was applied to the annual mean precipitation anomalies.

The reference evapotranspiration (ET0) was estimated by means of the empirical Hargreaves and Samani (HS) method (Hargreaves and Samani, 1985), using a *SPEI* package written in R language (Beguería et al. 2017). Vicente-Serrano et al. (2014) have shown that the HS method usually performed better than other empirical models. The HS method is based on the following expression:

$$ET0 = Re \cdot Ha(T + 17.8) \cdot \Delta T H_e \text{GMCs} \tag{3}$$

where H_a and H_e are empirical standard parameters; the H_a value is 0.0023 and the H_e value is 0.5. The solar radiation, R_e, is expressed in mm·day^{-1}. T is the mean temperature ((Tmax + Tmin)/2 in °C) and ΔT is the difference between Tmax and Tmin.

The standardized precipitation index (*SPI*) and the standardized precipitation evapotranspiration index (*SPEI*) are the most common drought indicators used in the Mediterranean

Basin. The *SPI* (McKee et al. 1993) is the most widely used index to quantify drought severity, and it is based on the assumption that rainfall variability is the main drought-driving factor. It is calculated on the total cumulative weekly (or monthly) precipitation data. *SPI* values usually span the range ± 3, where negative values indicate dry periods and positive values stand for wet periods (Stagge et al., 2015). By contrast, the *SPEI* (Vicente-Serrano et al. 2010), based upon the same calculation procedure used for the *SPI*, considers both precipitation and temperature. It assumes that water balance, expressed as the difference between precipitation and evapotranspiration, is the best drought identifier (Tirivarombo et al. 2018). Both indices are able to detect droughts at several timescales. This allows to compare the *SPEI* and *SPI* results over space and time.

In the following, the weekly *SPEI* and *SPI* values were estimated at 12-, 24-, and 36-month timescales for the selected GCM/RCM pairs. The main drought episodes were identified based on three conditions (Baronetti et al. 2020):

- Minimum duration of 3 consecutive weeks.
- Classification of drought episodes in heavy and extreme by means of thresholds. Heavy episodes were defined as those between the index value − 1.65 and − 1.28. Extreme episodes all the drought episodes characterised by an index value < − 1.65.
- Drought episodes have to affect at least 25% of the study area (González-Hidalgo et al. 2018).

Baseline (1971–2000), near future (2021–2050), and far future (2071–2100) drought events for RCP 4.5 and 8.5 were obtained identifying their magnitude, temporal duration, and percentage of affected area. The spatial distribution of the expected drought trends was checked using the Mann Kendall test (Mann, 1945), and a statistical significance of 95% was adopted. Finally, the spatial behaviour of drought duration according to *SPEI* and *SPI* was compared, based on the comparison between baseline climatic conditions (1971–2000) and future states expected respectively at global mean temperatures of + 2° and + 3 °C above preindustrial levels (Donnelly et al. 2017; Turco et al. 2018).

5 Results

5.1 Model validation and scaling factor estimate

The results of model validation indicated a precipitation overestimation by the models compared to the ground data, as reported in Table 2. Marked difference between model outputs and ground data are observed especially for the extreme event class. The pairs EC-EARTH-RACMO22E and MPI-ESM -CCLM4 provided the worse comparisons, with the highest Root Mean Square Error (*RMSE*) in the extreme event class (59.56 mm for the former and 56.11 mm for the latter), while the other GMC/RMC pairs gave *RMSE* that are no larger than 25.59 mm. In Table 2, the GCM/RCM pairs that are more biased in northern Italy are highlighted in grey. Table 3 reports the maximum and minimum temperature validation. In all cases, there was a clear bias of the model outputs to higher temperature values. This phenomenon is noticeable in the extreme cold and extreme warm classes, where the models significantly overestimated the temperature with *RMSE* values that range between 2.00 and 2.48 °C. The analysis of temperature differences did not identify GMC/RCM pairs that are more biased than others.

Table 2 Results of the model precipitation validation for the selected GCM/RCM pairs. For each precipitation class, the precipitation amount estimated by the models and recorded by the ground data and the corresponding *RMSE* are reported. The less reliable models are shaded in grey

	Class	Precipitation from models (mm)	Precipitation from ground stations (mm)	RMSE
EC-EARTH-RACMO22	weak	273.64	250.91	2.82
	mean	260.45	221.49	6.56
	heavy	153.68	146.45	6.29
	extreme	438.81	27.51	59.56
EC-EARTH-HIRHAM5	weak	240.67	239.78	2.40
	mean	156.83	139.15	6.41
	heavy	103.20	105.19	14.50
	extreme	527.01	430.62	25.59
MPI-ESM-CCLM4	weak	264.02	259.46	2.41
	mean	340.69	321.97	5.29
	heavy	202.28	165.49	10.06
	extreme	409.27	25.83	56.11
HadGEM2-CCLM4	weak	309.84	292.98	2.39
	mean	250.00	241.36	5.87
	heavy	182.01	145.27	10.58
	extreme	529.06	500.75	12.66
HadGEM2-RACMO22	weak	267.47	290.44	2.46
	mean	342.03	314.82	5.52
	heavy	259.80	219.24	10.46
	extreme	527.61	450.99	15.51
CM5-ALADIN52	weak	405.09	430.15	2.52
	mean	617.65	658.94	4.75
	heavy	91.87	82.28	9.02
	extreme	501.89	494.77	12.72

Figure 2a shows the spatial distribution of the scaling factors between ground data and GCM/RCM pairs for maximum and minimum temperature and for precipitation (further details on the performance of each model pair are given in Annex 1). For precipitation, values close to 0 indicate overestimation by the climate models, values close to 1 indicate agreement between simulations and ground data, and values larger than one represent underestimation by the GCM/RCM simulations. The precipitation scaling factors reported in Fig. 2a indicate a good agreement between simulations and ground data in the Po Plain and for the lowest parts of the Alpine chain. The standard deviations calculated for the ground data and for the models are also comparable in this area (Fig. 2b), and the scaling factors are no larger than the 0.3 times the GCM/RCMs standard deviation (Fig. 2c). However, for higher elevations in the Alps (Julian and Carnic Alps and western Alps), scaling

Table 3 Results of the model maximum and minimum temperature validation for the selected GCM/RCM pairs. For each temperature class, the average temperature estimated by the models and the ground data and the corresponding *RMSE* are reported

	Temperature	Class	Average temperature from models (°C)	Average temperature from ground stations (°C)	*RMSE*
EC-EARTH-RACMO22	Minimum temperature	Extr_Cold	− 2.25	− 3.82	2.43
		Cold	0.92	0.94	1.44
	Maximum temperature	Warm	28.70	28.14	1.63
		Extr_Warm	32.74	32.59	2.35
EC-EARTH-HIRHAM5	Minimum temperature	Extr_Cold	− 2.46	− 2.46	2.02
		Cold	1.15	1.44	1.44
	Maximum temperature	Warm	27.93	27.62	1.48
		Extr_Warm	31.70	31.14	2.26
MPI-ESM-CCLM4	Minimum temperature	Extr_Cold	− 1.52	− 1.77	2.00
		Cold	1.06	1.31	1.41
	Maximum temperature	Warm	28.36	27.83	1.70
		Extr_Warm	32.51	32.17	2.22
HadGEM2-CCLM4	Minimum temperature	Extr_Cold	− 0.85	− 2.80	2.52
		Cold	1.53	1.86	1.40
	Maximum temperature	Warm	27.98	27.56	1.67
		Extr_Warm	32.05	31.88	2.48
HadGEM2-RACMO22	Minimum temperature	Extr_Cold	− 1.01	− 0.73	0.91
		Cold	2.40	3.80	2.13
	Maximum temperature	Warm	28.07	27.61	1.61
		Extr_Warm	32.50	31.70	2.44
CM5-ALADIN52	Minimum temperature	Extr_Cold	− 7.00	− 8.44	2.15
		Cold	− 3.83	− 4.50	1.58
	Maximum temperature	Warm	24.66	24.80	1.08
		Extr_Warm	31.38	30.10	2.33

factors close to zero are detected. For the Ligurian region and the southern portion of the Po Plain, on the other hand, scaling factors larger than 1 are present.

For temperature, values close to 0 °C indicate agreement between simulations and ground data, negative values indicate overestimation by the GCM/RCM simulations while positive values imply underestimation by the GCM/RCM simulations. In Fig. 2a, the spatial distribution of the scaling factors shows that the Po Valley and the foothills have the best agreement between simulated and measured temperatures. For maximum and minimum temperature, the scaling factors are between − 2 and + 2 °C. Figure 2b also shows that the standard deviations calculated on the simulated and ground data are comparable in this area; the scaling factors are up to 5 times the GCM/RCMs standard deviation (Fig. 2c). Model overestimation is observed for the southern part of the study area with scaling factors for maximum temperature of about − 2 °C and -4 °C. In a few areas along the western Ligurian coast, scaling factors between − 4 and − 6 °C were detected. The underestimation is mainly located in the eastern Alps (Julian and Carnic Alps) and western Alps, with scaling factors from about 4 to 6 °C for maximum and minimum temperature.

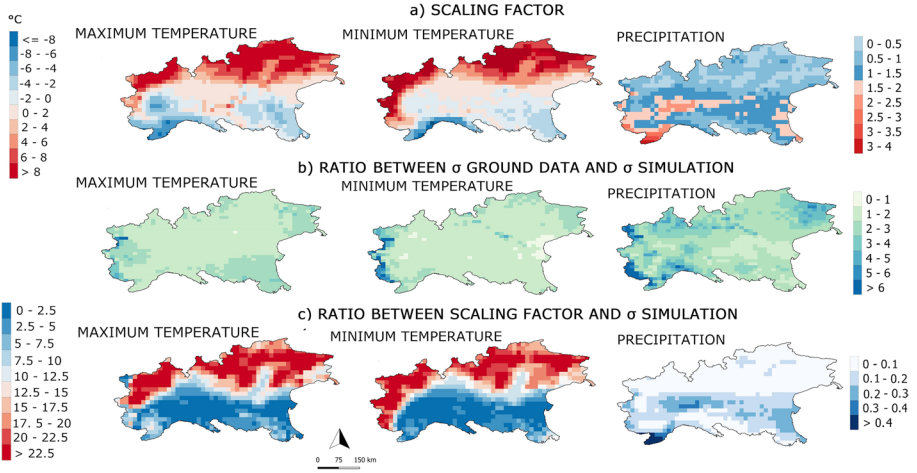

Fig. 2 GCM/RCM pairs validation in northern Italy. Figure shows **a** scaling factors for bias correction, estimated for maximum and minimum temperature and for precipitation; **b** ratio between standard deviations calculated from ground data and the GCM/RCM pairs; **c** ratio between the bias scaling factor and the GCM/RCMs standard deviation

5.2 Precipitation and temperature anomalies

Figure 3 shows the ensemble average for the near (2021–2050) and far (2071–2100) future mean annual temperature and precipitation anomalies in northern Italy for the RCP 4.5 and 8.5 scenarios (further details on the performance of each model pair are provided in Annexes 2, 3, and 4). An increase of minimum and maximum temperature is evident for the whole study area, with a more complex behaviour of precipitation anomalies.

For the near future, both scenarios indicate that the Alpine chain will be significantly affected by global warming, with annual maximum temperature anomalies between 3 and 4 °C and annual minimum temperature anomalies from 2 to 3 °C (Fig. 3a). In the same period, the Po Valley and coastal areas will experience no more than 2 °C of temperature increase. For precipitation, Fig. 3c shows that for RCP 4.5 most of the study area is expected to be interested by very small precipitation changes (anomalies close to 0 mm),

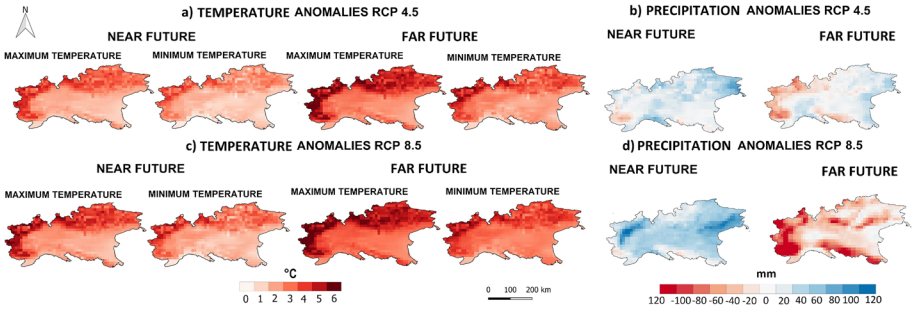

Fig. 3 Ensemble averages of precipitation and maximum and minimum temperature anomalies estimated in northern Italy. Figure shows the following: **a** near future temperature anomalies under the RCP 4.5 and RCP 8.5; **b** far future temperature anomalies under the RCP 4.5 and RCP 8.5; **c** near future precipitation anomalies under the RCP 4.5 and RCP 8.5; **d** far future precipitation anomalies under the RCP 4.5 and RCP 8.5

while the Ligurian coast and the eastern Alps display positive precipitation anomalies of about 40 mm. A stronger precipitation increase is instead obtained for RCP 8.5 in the western and Julian Alps (anomalies between 80 and 120 mm).

For the last 30 years of the twenty-first century, the modelled temperature anomalies display the same spatial behaviour observed for the near future (Fig. 3b) with annual maximum temperature anomalies between 4 and 6 °C and annual minimum temperature anomalies between 3 and 4 °C in the Alps. In the Po Plain, and especially along the Ligurian coast, the temperature anomalies will not exceed 3 °C. For precipitation, the eastern portion of the Alps (Carnic and Julian Alps) is expected to experience a precipitation increase of about 40 mm, while the western Alps will be affected by a decrease of precipitation (anomalies of − 40 mm). The RCP 8.5 scenario shows an intensification of this tendency, with negative annual precipitation anomalies in the entire Alpine chain, and anomalies of − 80 mm in the western Alps (Fig. 3d). Overall, these results indicate an unchanged, or slightly increasing, precipitation in the Alps for the near future, followed by a significant precipitation decrease at the end of the century. The RCP 4.5 and RCP 8.5 scenarios provide qualitatively analogous results, with the RCP 8.5 case showing enhanced changes.

5.3 Drought estimates

Figure 4 shows the statistics of extreme drought episodes for the baseline (1971–2000), near (2021–2050), and far (2071–2100) future 30-year periods as identified by *SPEI* and *SPI* at the 12-month timescale, for RCP 4.5 and RCP 8.5. The plain-coloured histograms represent the *SPEI* results, while the line pattern marks the *SPI* outcomes. For each combination of RCM and GMC, the figure reports the total number, the mean percentage of affected area, and the mean duration of the drought events for the considered 30-year period. Overall, Fig. 4 indicates that the *SPEI* and *SPI* detect the same number of drought events, with somehow different results in the percentage of affected area and drought duration. The drought analysis based on *SPEI* indicates that for the baseline period (1971–2000), 3 to 5 extreme drought events are identified. In the period 2021–2050, an increase of extreme drought events is present for the RCP 8.5 scenario, with 5 to 8 extreme drought events (Fig. 4b). For the far future (2071–2100), the number of severe drought episodes is expected to further increase for the majority of the reliable model pairs and for both scenarios.

The percentage of area affected by droughts is reported in Fig. 4, showing that in the 1971–2000 period, the maximum percentage of area involved by an extreme drought event ranged between 32 and 47%. For the concentration pathway RCP 4.5 in the 2021–2050 period, the maximum percentage of area interested by an extreme drought event is expected to be comparable with that of the baseline period. On the other hand, an increase of the drought-affected area is expected for the last 30 years of the century, with a maximum of 55% of interested area during a single episode as simulated by the pair HadGEM2-RACMO22E for the RCP 4.5 scenario. This percentage is even larger in RCP 8.5, with 68% estimated by the same pair.

The maximum duration of the main drought events ranges from 13 to 25 weeks for the 1971–2000 period (Fig. 4). An increase of drought duration is detected for the near future in the RCP 4.5 scenario, with maximum duration ranging from 15 consecutive weeks for the CM5-ALADIN52 pair to 29 weeks for EC-EARTH-HIRHAM5. A further increase is expected for the last 30 years of the century; for the period 2071–2100, the maximum

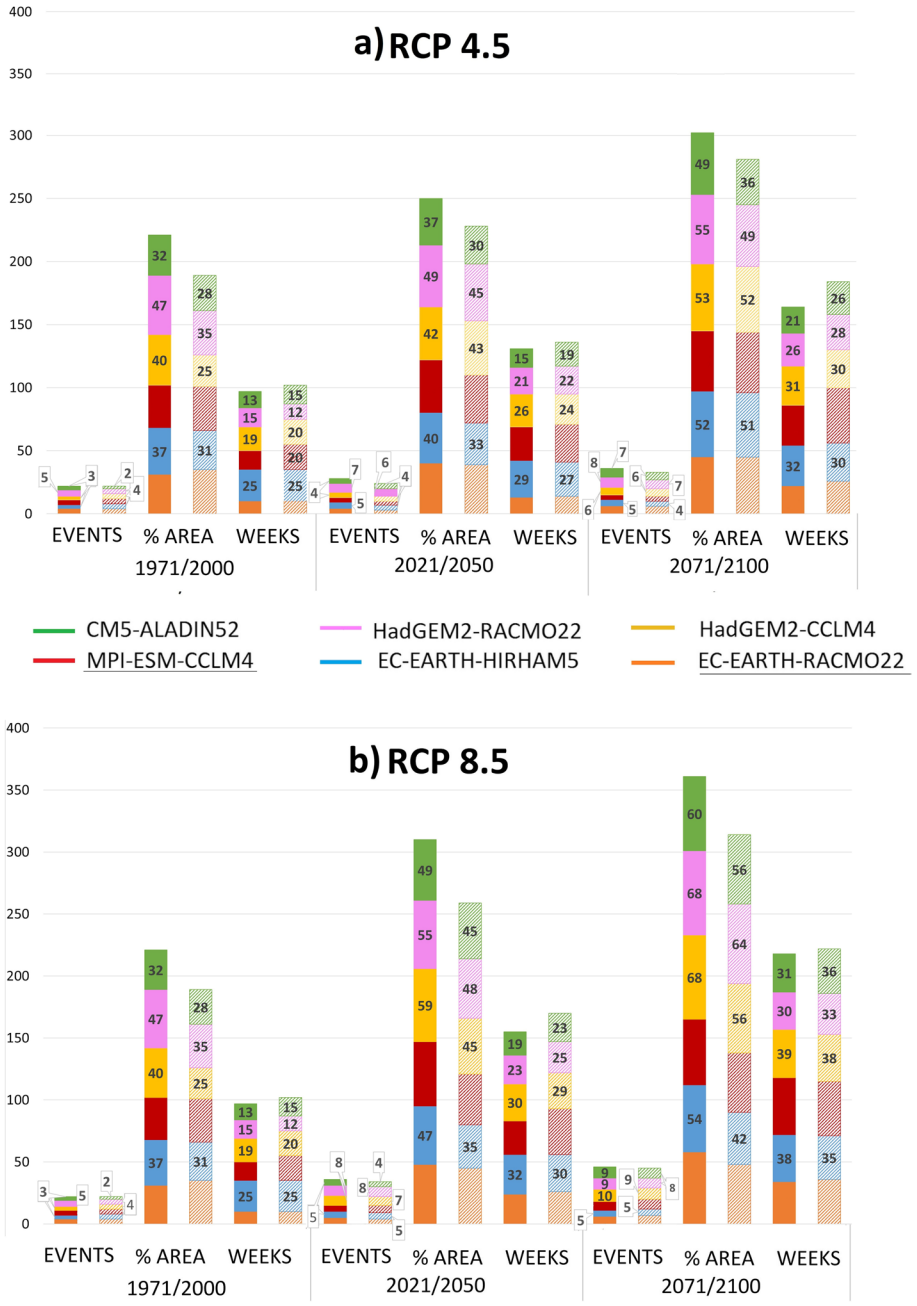

Fig. 4 Number of drought events, mean percentage of area affected by drought and mean number of consecutive drought weeks expected for the baseline (1971–2000), near (2021–2050), and far future (2071–2100). Colors identify different model pairs as indicated in the legend. Plain-coloured histogram represents 12-month *SPEI* results, and line patterns indicate 12-month *SPI* results. The less reliable models are underlined and values were not provided

duration will be between 21 and 32 weeks, respectively estimated by CM5-ALADIN52 and EC-EARTH-HIRHAM5 in the RCP 4.5 scenario. Similar results, with larger changes, are obtained for RCP 8.5.

The comparison between the two drought indices calculated at 12-, 24-, and 36-month timescale, for the baseline, near, and far future periods is reported in Fig. 5. Positive values stand for *SPEI*-identified episodes that are more extended than those identified by *SPI*. In 1971–2000, for all GMC/RCM pairs, there is a tendency of *SPEI* to detect drought events that are more extended than for *SPI*; at 36-months *SPEI* detects events that are 25% and 30% more extended than those estimated by *SPI* (Fig. 5a). Consistently, in 2021–2050, for all GMC/RCM pairs, *SPEI* detects more severe drought events than *SPI* (Fig. 5b). This happens for all the timescales of integration; in particular at 36-months, the events detected by *SPEI* are 17% and 25% more extended that for *SPI*. For the 2071–2100 period, the difference between *SPEI* and *SPI* is more varied, and it was not possible to detect a consistent difference between the two indices (Fig. 5c).

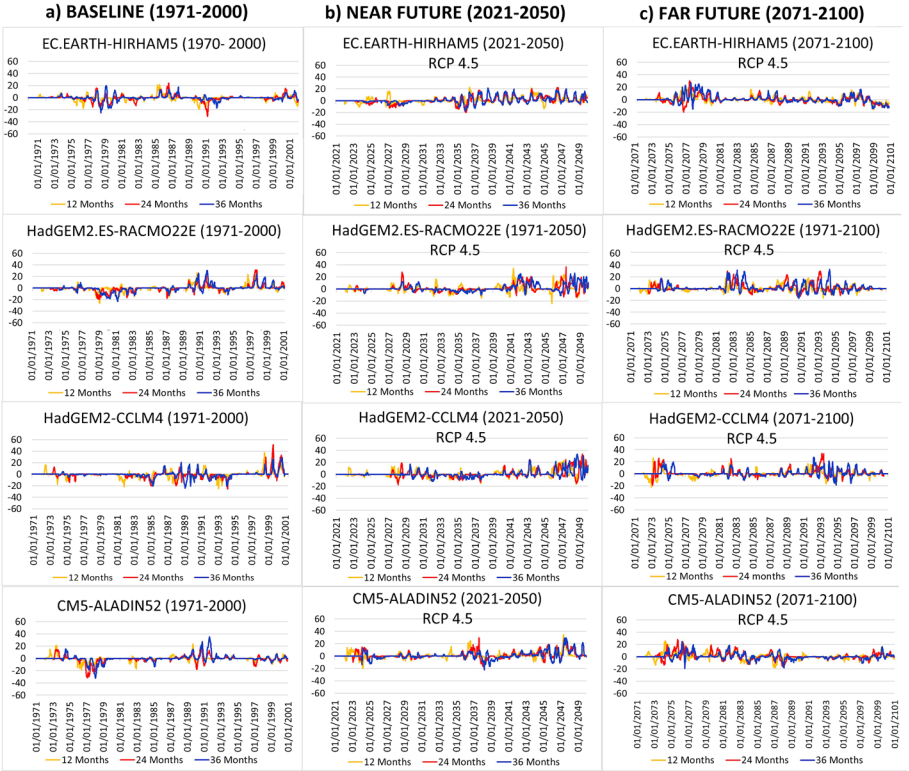

Fig. 5 Difference in the percentage of area affected by intense drought events as estimated by *SPEI* and *SPI* for RCP 4.5, as a function of time for the following: **a** baseline period (1971–2000); **b** near future (2021–2050); **c** far future (2071–2100). Model pairs are indicated in the legends. The blue lines stand for a temporal aggregation scale of 12 months, orange is for 24 months, and black is for 36 months

5.4 Drought trends and spatial behaviour

The analysis of the most intense drought events identified an increase of severity in the 2071–2100 period, in terms of both the duration and percentage of drought-affected area. Figure 6 reports the 12-month *SPEI* trends and their statistical significance in the 2021–2100 period for RCP 4.5 and RCP 8.5, for the four most reliable GCM/RCM pairs. For RCP 4.5 (Fig. 6a), HadGEM2-CCLM4, HadGEM2-RACMO22, and CM5-ALADIN52 show a significant intensification of droughts along the Alpine chain. In this area, the drought index is expected to decrease between − 1.2 and − 1.8 $\Delta SPEI$/30 years. In other parts of northern Italy, the three model pairs indicate no significant and close to zero trend

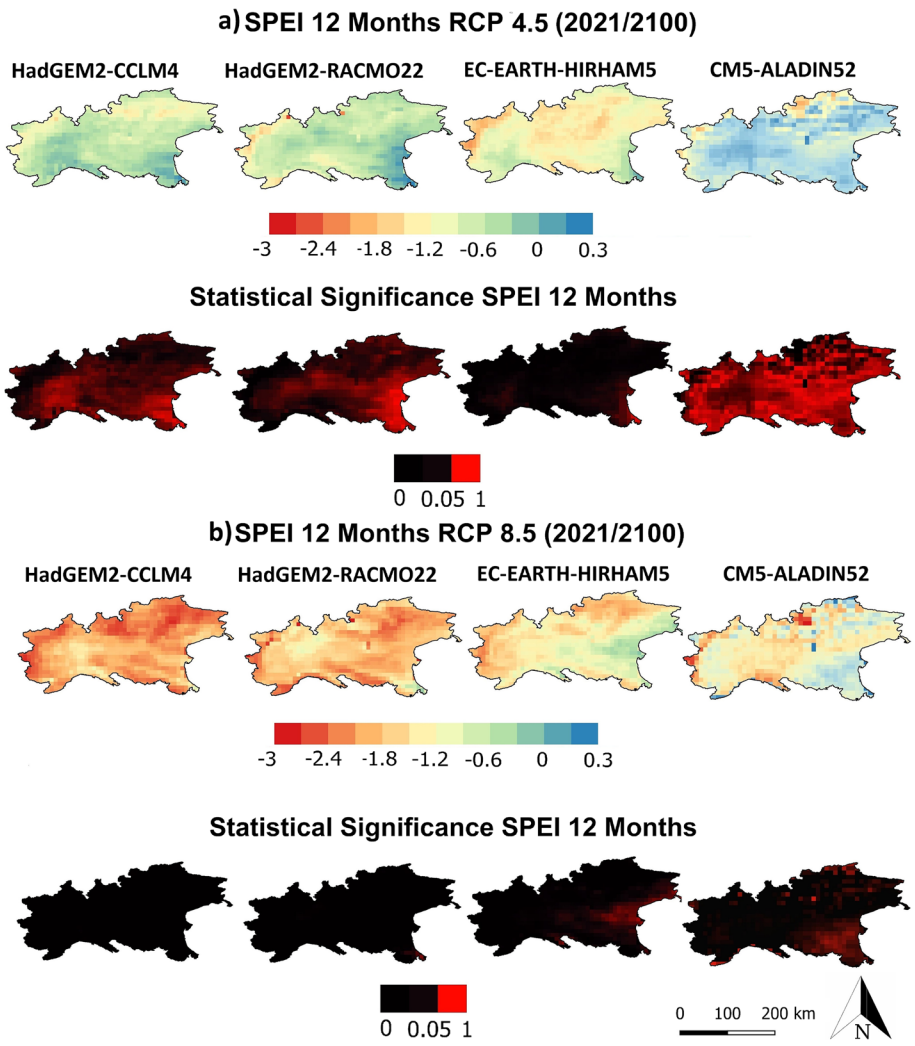

Fig. 6 Spatial distribution and statistical significance of the 12-month *SPEI* trends for the 2021–2100 period in northern Italy for the following: **a** RCP 4.5 scenario, **b** RCP 8.5 scenario. The four most reliable model pairs are shown

for the 2021–2100 period, while EC-EARTH-HIRHAM5 indicates a significant increase of droughts also for the central portion (North of the Po Plain, − 1.8 *ΔSPEI*/30 years). For RCP 8.5, the models estimate an increase of drought severity (Fig. 6b). For HadGEM2-CCLM4 and HadGEM2-RACMO22, the analysis showed significant trends for the whole study area, which becomes especially intense in the Alps (2.4 and -3 *ΔSPEI*/30 years).

The change in the spatial extent of drought episodes, compared to the baseline condition, was investigated considering also how droughts develop in case of a global warming of + 2 or + 3 °C above preindustrial levels, in keeping with the recent IPCC approach. Figure 7 shows the spatial extent of heavy and extreme drought events according to *SPEI* and *SPI* at 12 months. In northern Italy, heavy drought events are homogenously distributed in the 1971–2000 period with duration between 6 and 8 consecutive weeks. Longer extreme drought episodes are detected by *SPI* in the Alps (8 to 10 weeks, Fig. 7a). Both indicators reveal that, for a global temperature increase of + 2 °C, heavy drought events will be present in the study area, with duration from 5 to 15 consecutive weeks. In a few sectors along the Alps, extreme drought events with a duration of 20 weeks are also foreseen (Fig. 7b). Moving to a + 3 °C global temperature increase, no relevant enhancement of heavy drought events is observed. On the opposite, extreme drought episodes show a strong increase. In particular, the southern portion of the Po Plain is expected to experience extreme droughts with duration of 30 consecutive weeks (Fig. 7c). Once more, the difference in climate change impacts between + 2 and + 3 °C is striking.

6 Discussion

6.1 Model validation and scaling factors estimate

Model validation was performed for the six historical GCM/RCM pairs in the period 1971–2000. The results provided by the innovative use of Co.Rain and Co.Temp software algorithms evidenced a well-defined model overestimation of the extreme event class. Moreover, the applied methodology indicated that, among the selected simulations, the pairs EC-EARTH-RACMO22E and MPI-ESM-CCLM4 provided the worse comparisons with the observations.

The investigation of the precipitation and temperature annual scaling factors for northern Italy showed a good agreement between measured and simulated values in the Po Valley, while in mountain regions and coastal areas, the simulations are affected by considerable uncertainty. Precipitation overestimation and temperature underestimation were detected in proximity of the Carnian and Julian Alps (north-eastern Italy). This is one of the wettest sectors of northern Italy and its climate is strongly influenced by the Scirocco and Libeccio winds, which are two moist and mild flows coming from respectively South-East and South-West (Fratianni and Acquaotta 2017).

Underestimation of precipitation and overestimation of temperature by GCM/RCM pairs are observed in proximity of the Ligurian coast. The climate of this area is strongly affected by mesoscale convective patterns generated over the sea, because of the convergence between cold and dry flows coming from the North and warm and wet south-easterly flow. The interaction between these circulations and orography generates heavy precipitation events for prolonged periods (Fiori et al. 2017; Parodi et al. 2017).

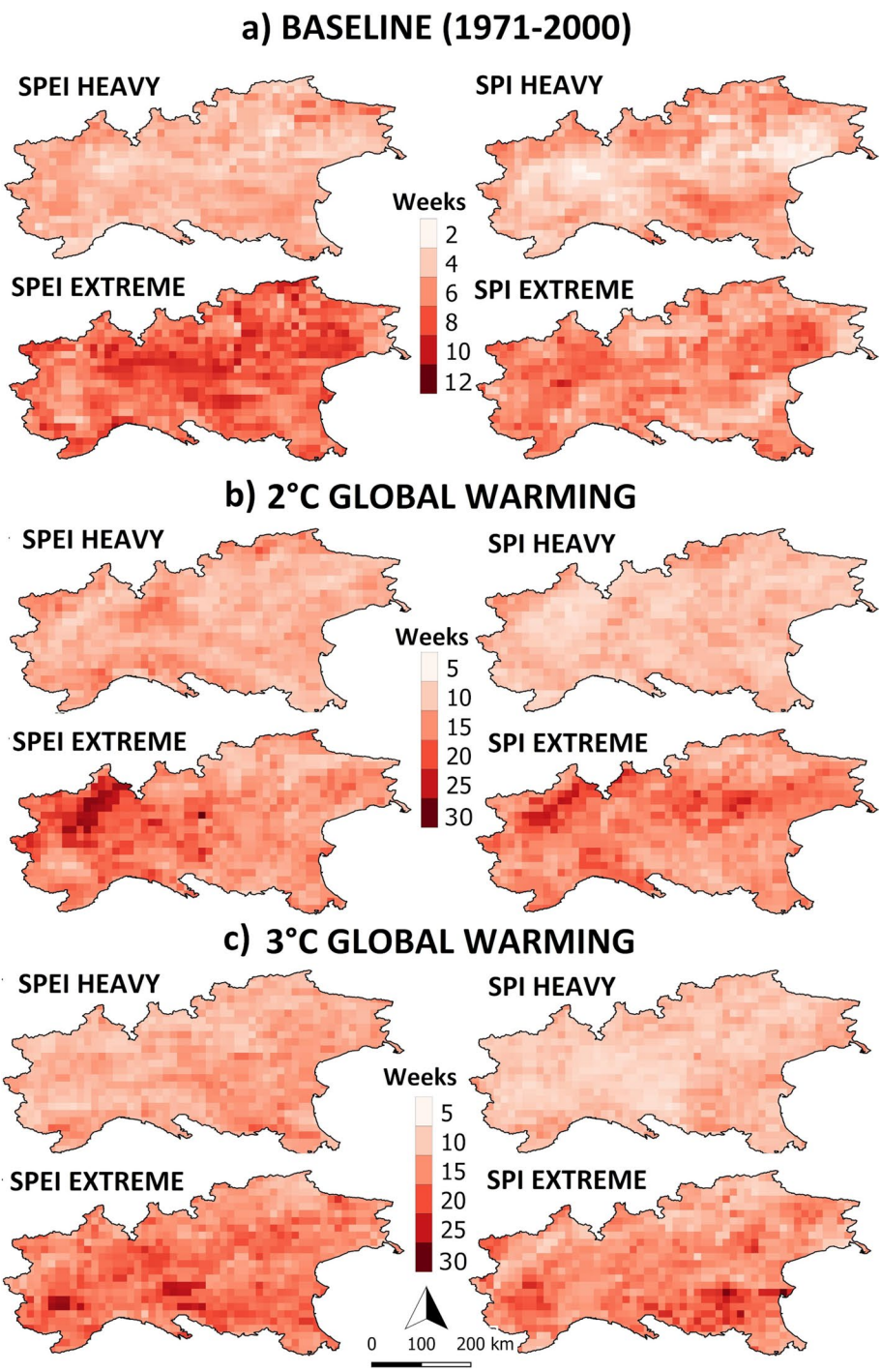

Fig. 7 Spatial distribution of drought duration (in consecutive weeks) for "heavy" and "extreme" events (see text for definition), computed from *SPI* and *SPEI*: **a** baseline period (1971–2000); **b** global warming of + 2 °C; **c** global warming of + 3 °C

6.2 Precipitation and temperature anomalies

The model results indicate a significant warming in the Alpine chain for the 2021–2050 period. This outcome is consistent with the study of Zimmermann et al. (2013) which found that, for the first 50 years of this century, the Alps will face higher warming trends with respect to the neighbouring sectors. Warming in the mountains is expected to continue in the last 30 years of the century, and this will be more marked in summer (Gobiet et al. 2014). This will be reflected in enhanced glacier volume loss, estimated to be about 80–90% by the end of the century for RCP 4.5 (Radić et al. 2014).

Future precipitation anomalies are less clear than temperature changes. The models indicate that most of northern Italy is expected to experience only small precipitation changes, except for some regions (western and Julian Alps) with moister conditions in the near future, see also Brussolo et al. (2022) for a study of climate-induced hydrological changes in north-western Italy.

6.3 Drought estimates

The comparison of future drought characteristics with the reference period (1971–2000) indicated that an increase in the percentage of affected area and drought duration will occur for the last 30 years of the twenty-first century, while the number of drought events remained approximately constant.

The application of *SPEI* and *SPI* has revealed a high complexity of the individual drought events: both indices were able to detect the same drought events, but marked differences were present in the estimated percentage of drought-affected area, suggesting that droughts may depend on different triggering factors (Trenberth et al. 2013). During the 1971–2000 period, most GCMs/RCMs pairs indicated that drought episodes appear to be related to an above-normal evaporative demand. This is presumably linked with the significant positive temperature trends observed by Acquaotta et al. (2015) for 1961–2010 in Piedmont (northern Italy). Analogous results were obtained also for the near future (2021–2050), and Marcos-Garcia et al. (2017) suggested that the increase of temperature will play the most important role in future drought episodes in the first half of this century. On the contrary, for the far future (2071–2100), the relation between the two drought indices is not clear. Several studies (e.g. Merkenschlage and Hertig, 2020 and Brogli et al. 2019) found that winter precipitation quantiles are expected to decrease at the end of the century in the whole Mediterranean area. More extended dry periods and extreme precipitation episodes are also expected, associated with drier conditions during summer.

6.4 Drought trends and spatial behaviour

This study provided, for the first time, drought spatial distribution maps for the whole of northern Italy. The trend analysis indicated that the entire Alpine Range, characterised by the rainiest and snowiest areas (Diodato et al. 2021 and Terzago et al. 2012), will also experience an increase in drought severity in the RCP 4.5 scenario.

For a + 2 °C increase of global temperature, extreme drought episodes will be characterised by very long dry spells in the Alps. This implies potentially severe impacts on permafrost degradation, influencing surface water quality, erosion and slope instability (Colombo et al. 2019). For a + 3 °C increase of global temperature, a North-to-South gradient of dry spells is identified, and the Po Plain will become more severely affected by extremely long

drought events. Long dry periods have a marked impact on agriculture: as a consequence of a large number of consecutive dry days, there can be a significant reduction of crop yield (Raymond et al. 2019). In northern Italy, current drought episodes are mostly influenced by the North Atlantic Oscillation (NAO) and the Mediterranean Oscillation (MO), associated with the North-to-South propagation gradient (Baronetti et al. 2020). This drought gradient, estimated also for the twenty-first century, is probably the result of a stronger positive phase of NAO and MO, leading to drier conditions over northern Italy and most of the Mediterranean basin. Santos et al. (2007) estimated a future extension of the NAO's southern centre of action through the eastern part of the Mediterranean Basin, implying an intensification of NAO effects in southern Europe. This difference between the positive and negative phase of NAO can rationalize the expected, future North-to-South drought gradient and the decrease of precipitation for the last decades of the century.

7 Conclusions

This work analysed the expected properties of drought episodes in the near (2021–2050) and far (2071–2100) future compared to the baseline conditions (1971–2000) for northern Italy, a crucial region from the point of view of water resources and European economy. EURO-CORDEX and MED-CORDEX GCMs/RCMs pairs at spatial resolution of 0.11 degrees were analysed for the RCP 4.5 and RCP 8.5 concentration pathways. To increase the reliability of the results, model validation was addressed applying, for the first time, the Co.Rain and Co.temp software algorithms, revealing that all model pairs tended to overestimate precipitation and temperature extreme events, and the pairs EC-EARTH-HIRHAM5, HadGEM2-CCLM4, HadGEM2-RACMO22, and CM5-ALADIN52 performed best for northern Italy. Such validation procedure provided estimates of the precipitation and temperature scaling factors which could be used in linear bias correction techniques, albeit they were not directly employed here as we compared model projections with model baseline (i.e., anomalies). The results indicated that the Po Valley and the foothills are the areas where the GCM/RCM pairs performed best, while in complex environments such as coastal areas and mountain regions, the simulations were affected by considerable uncertainty.

The results of the analysis indicated that, although northern Italy is historically rich in water resources, the trend towards dry conditions already observed in 1971–2000 will continue in the twenty-first century. Most GCM/RCM pairs indicated an increase of drought severity, in terms of duration and percentage of drought-affected area, especially for RCP 8.5 and for the later part of the century. In particular, the Alpine area (a water tower for the surrounding area) will be significantly affected by higher positive temperature anomalies and increasing drought conditions.

This study also indicated the importance of adopting multiple drought indices, as the comparison revealed that only one index does not tell the full story. A positive evapotranspiration anomaly appeared to be the main drought-triggering factor for the baseline situation and for the first part of the century. Finally, spatial distribution maps of drought events were provided for northern Italy, showing that the Alpine chain is the most sensitive area in northern Italy.

Supplementary Information The online version contains supplementary material available at https://doi.org/10.1007/s10584-022-03370-7.

Acknowledgements This study was carried out under the PhD fellowship founded by the University of Turin, Italy. The authors thank Renan Le Roux of the Environments and Societies Department of CIRAD (Montpellier, France) and Nicola Colombo of the University of Turin for their help in the data rescue.

Author contribution All authors contributed to the study concept and design. Material preparation, data collection, and analysis were performed by AB. AB drafted the manuscript, with a substantial contribution from VD, AP, and SF.

Funding This work was also partially funded by the project Erasmus Traineeships + (University of Turin, Italy, I TORINO01).

Declarations

Competing interests The authors declare no competing interests.

References

Acquaotta F, Fratianni S, Garzena D (2015) Temperature changes in the North-Western Italian Alps from 1961 to 2010. Theor Appl Climatol 122(3–4):619–634. https://doi.org/10.1007/s00704-014-1316-7

Baronetti A, González-Hidalgo JC, Vicente-Serrano SM, Acquaotta F, Fratianni S (2020) A weekly spatio-temporal distribution of drought events over the Po Plain (North Italy) in the last five decades. Int J Climatol 40(10):4463–4476. https://doi.org/10.1002/joc6467

Beguería S, Vicente-Serrano SM, Beguería MS (2017) Package 'SPEI'. Calculation of the standardised precipitation-evapotranspiration index. Available at: https://cran.r-project.org/web/packages/SPEI/SPEI.pdf. (Accessed 31/03/2022)

Bigi A, Ghermandi G, Harrison RM (2012) Analysis of the air pollution climate at a background site in the Po valley. J Environ Monit 14(2):552–563. https://doi.org/10.1039/C1EM10728C

Brogli R, Sørland SL, Kröner N, Schär C (2019) Causes of future Mediterranean precipitation decline depend on the season. Environ Res Lett 14(11):114017. https://doi.org/10.1088/1748-9326/ab4438

Brunner MI, BjörnsenGurung A, Zappa M, Zekollari H, Farinotti D, Stähli M (2019) Present and future water scarcity in Switzerland: potential for alleviation through reservoirs and lakes. Sci Total Environ 666:1033–1047. https://doi.org/10.1016/j.scitotenv.2019.02.169

Brussolo E, Palazzi E, von Hardenberg J, Masetti G, Vivaldo G, Previati M, Canone D, Gisolo D, Bevilacqua I, Provenzale A, Ferraris S (2022) Aquifer recharge in the Piedmont Alpine zone: historical trends and future scenarios. Hydrol Earth Syst Sci 26:407–427. https://doi.org/10.5194/hess-26-407-2022

Colmet-Daage A, Sanchez-Gomez E, Ricci S, Llovel C, BorrellEstupina V, Quintana-Seguí P, Llasat MC, Servat E (2018) Evaluation of uncertainties in mean and extreme precipitation under climate change for northwestern Mediterranean watersheds from high-resolution Med and Euro-CORDEX ensembles. Hydrol Earth Syst Sci 22(1):673–687. https://doi.org/10.5194/hess-2017-49

Colombo N, Salerno F, Martin M, Malandrino M, Giardino M, Serra E, Godone D, Said-Pullicino D, Fratianni S, Paro L, Tartari G, Freppaz M (2019) Influence of permafrost, rock and ice glaciers on chemistry of high-elevation ponds (NW Italian Alps). Sci Total Environ 685:886–901. https://doi.org/10.1016/jscitotenv201906233

Critto A, Torresan S, Ronco P, Zennaro F, Santini M, Trabucco A, Marcomini A (2016) Assessing hydrological drought risk for the irrigation sector in future climate scenarios: lessons learned from the Apulia case study (Italy). EGU Abstracts. 2016EGUGA187813C

D'Andrea F, Provenzale A, Vautard R, De Noblet-Decoudré N (2006) Hot and cool summers: Multiple equilibria of the continental water cycle. Geophys Res Lett 33(24):1–6. https://doi.org/10.1029/2006GL027972

Desiato F, Fioravanti G, Fraschetti P, Perconti W, Piervitali E (2015) Il clima futuro in Italia: analisi delle proiezioni dei modelli regionali. ISPRA 58https://doi.org/10.1017/CBO9781107415324004

Diodato N, Gómara I, Baronetti A, Fratianni S, Bellocchi G (2021) Reconstruction of erosivity density in northwest Italy since 1701. Hydrol Sci J 66(7):1185–1196. https://doi.org/10.1080/02626667.2021.1918696

Diodato N, Fratianni S, Bellocchi G (2020) Reconstruction of snow days based on monthly climate indicators in the Swiss pre-alpine region. Reg Environ Change 20:55. https://doi.org/10.1007/s10113-020-01639-0

Donnelly C, Greuell W, Andersson J, Gerten D, Pisacane G, Roudier P, Ludwig F (2017) Impacts of climate change on European hydrology at 15, 2 and 3 degrees mean global warming above preindustrial level. Clim Change 143(1–2):13–26. https://doi.org/10.1007/s10584-017-1971-7

Dubreuil V (1997) La sécheresse dans la France de l'Ouest : une contrainte climatique trop souvent oubliée. Sci Chang Planét Sécher 8(1):47–55

Drumond A, Gimeno L, Nieto R, Trigo RM, Vicente-Serrano SM (2017) Drought episodes in the climatological sinks of the Mediterranean moisture source: the role of moisture transport. Glob Planet Change 151:4–14. https://doi.org/10.1016/jgloplacha201612004

Fang G, Yang J, Chen YN, Zammit C (2015) Comparing bias correction methods in downscaling meteorological variables for a hydrologic impact study in an arid area in China. Hydrol Earth Syst Sci 19(6):2547–2559. https://doi.org/10.5194/hessd-11-12659-2014

Farinotti D, Pistocchi A, Huss M (2016) From dwindling ice to headwater lakes: could dams replace glaciers in the European Alps? Environ Res Lett 11(5):054022. https://doi.org/10.1088/1748-9326/11/5/054022

Fiori E, Ferraris L, Molini L, Siccardi F, Kranzlmueller D, Parodi A (2017) Triggering and evolution of a deep convective system in the Mediterranean Sea: modelling and observations at a very fine scale. Q J Roy Meteor Soc 143(703):927–941. https://doi.org/10.1002/qj2977

Fratianni S, Acquaotta F (2017) The climate of Italy. In: Soldati M, Marchetti M (eds) Landscapes and Landforms of Italy, 1s edn. Springer International Publishing, Swiss, pp 29–30 https://doi.org/10.1007/978-3-319-26194-2_4

Fratianni S, Cassardo C, Cremonini R (2009) Climatic characterization of Foehn episodes in Piedmont Italy. Geogr Fis Din Quat 32:5–22. ISSN 0391–9838

Gandolfi C, Facchi A, Crespi A, Rienzner M, Maugeri M (2019) Drought variability and trend over the Lombardy plain from meteorological station records. In: International Mid-Term Conference of the Italian Association of Agricultural Engineering, Springer, pp 39–47

García-Herrera R, Garrido-Perez JM, Barriopedro D, Ordóñez C, Vicente-Serrano SM, Nieto R, Gimeno L, Sorí R, Yiou P (2019) The European 2016/17 drought. J Clim 32:3169–3187. https://doi.org/10.1175/JCLI-D-18-0331.1

Ghimire U, Srinivasan G, Agarwal A (2019) Assessment of rainfall bias correction techniques for improved hydrological simulation. Int J Climatol 39(4):2386–2399. https://doi.org/10.1002/joc5959

Gobiet A, Kotlarski S, Beniston M, Heinrich G, Rajczak J, Stoffel M (2014) 21st century climate change in the European Alps-A review. Sci Tot Env 493:1138–1151. https://doi.org/10.1016/jscitotenv201307050

González-Hidalgo JC, Vicente-Serrano SM, Peña-Angulo D, Salinas C, Tomas-Burguera M, Beguería S (2018) High resolution spatio-temporal analyses of drought episodes in the western Mediterranean basin (Spanish mainland, Iberian Peninsula). Acta Geophysi 66:81–392. https://doi.org/10.1007/s11600-018-0138-x

Guenzi D, Acquaotta F, Garzena D, Baronetti A, Fratianni S (2019) An algorithm for daily temperature comparison: CoTemp-comparing series of temperature. Earth Sci Inform 13:205–210. https://doi.org/10.1007/s12145-019-00414-y

Guenzi D, Acquaotta F, Garzena D, Fratianni S (2017) CoRain: a free and open source software for rain series comparison. Earth Sci Inform 10(3):405–416. https://doi.org/10.1007/s12145-017-0301-y

Hargreaves GH, Samani ZA (1985) Reference crop evapotranspiration from temperature. Appl Eng Agric 1(2):96–99

IPCC, 2022: Summary for Policymakers [H-O Pörtner, DC Roberts, ES Poloczanska, K Mintenbeck, M Tignor, A Alegría, M Craig, S Langsdorf, S Löschke, V Möller, A Okem (eds.)]. In: Climate Change 2022: Impacts, Adaptation, and Vulnerability. Contribution of Working Group II to the Sixth Assessment Report of the Intergovernmental Panel on Climate Change [H-O Pörtner, DC Roberts, M Tignor, ES Poloczanska, K Mintenbeck, A Alegría, M Craig, S Langsdorf, S Löschke,

V Möller, A Okem, B Rama (eds.)]. Cambridge University Press. In PressJacob D, Petersen J, Eggert B et al (2014) EURO-CORDEX: new high-resolution climate change projections for European impact research. Reg Environ Change 14:563–578. https://doi.org/10.1007/s10113-013-0499-2

Lamy C, Dubreuil V (2013) Impact potentiel du changement climatique sur les sécheresses pédologiques en Bretagne au 21eme siècle. Climatologie 10:107–121. https://doi.org/10.4267/climatologie.96

Lopez-Bustins JA, Pascual D, Pla E, Retana J (2013) Future variability of droughts in three Mediterranean catchments. Nat Hazards 69(3):1405–1421. https://doi.org/10.1007/s11069-013-0754-3

Luterbacher J, Dietrich D, Xoplaki E, Grosjean M, Wanner H (2004) European seasonal and annual temperature variability, trends, and extremes since 1500. Science 303:1499–1503. https://doi.org/10.1126/science.1093877

Mann HB (1945) Nonparametric tests against trend. Econometrica 13:245–259

Manzano A, Clemente MA, Morata A, Luna MY, Beguería S, Vicente-Serrano SM, Martín ML (2019) Analysis of the atmospheric circulation pattern effects over SPEI drought index in Spain. Atmos Res 230:104630. https://doi.org/10.1016/j.atmosres.2019.104630

Marcos-Garcia P, Lopez-Nicolas A, Pulido-Velazquez M (2017) Combined use of relative drought indices to analyze climate change impact on meteorological and hydrological droughts in a Mediterranean basin. J Hydrol 554:292–305. https://doi.org/10.1016/jjhydrol201709028

McKee TB, Doesken NJ, Kleist J (1993) The relationship of drought frequency and duration to timescales. In: Proceedings of the 8th Conference on Applied Climatology. American Meteorological Society, Boston, pp 179–184

Merkenschlager C, Hertig E (2020) Seasonal assessments of future precipitation extremes in the Mediterranean area considering non-stationarities in predictor-predictand relationships. Clim Res 80(1):19–42. https://doi.org/10.3354/cr01590

Mishra AK, Singh VP (2010) A review of drought concepts. J Hydrol 391(1–2):202–216. https://doi.org/10.1016/jjhydrol201007012

Nigrelli G, Fratianni S, Zampollo A, Turconi L, Chiarle M (2018) The altitudinal temperature lapse rates applied to high elevation rockfalls studies in the Western European Alps. Theor Appl Climatol 131(3–4):1479–1491. https://doi.org/10.1007/s00704-017-2066-0

Parodi A, Ferraris L, Gallus W, Maugeri M, Molini L, Siccardi F, Boni G (2017) Ensemble cloud-resolving modelling of a historic backbuilding mesoscale convective system over Liguria: the San Fruttuoso case of 1915. Clim Past 13:455–472. https://doi.org/10.5194/cp-13-455-2017

Radić V, Bliss A, Beedlow AC et al (2014) Regional and global projections of twenty-first century glacier mass changes in response to climate scenarios from global climate models. Clim Dyn 42:37–58. https://doi.org/10.1007/s00382-013-1719-7

Raymond F, Ullmann A, Tramblay Y, Drobinski P, Camberlin P (2019) Evolution of Mediterranean extreme dry spells during the wet season under climate change. Reg Environ Change 1-13https://doi.org/10.1007/s10113-019-01526-3

Ruti P, Somot S, Giorgi F et al (2015) MED-CORDEX initiative for Mediterranean climate studies. Bull Amer Meteor Soc 97(7):1187–1208. https://doi.org/10.1175/BAMS-D-14-001761

Santos JA, Corte-Real J, Ulbrich U, Palutikof J (2007) European winter precipitation extremes and large-scale circulation: a coupled model and its scetolnarios. Theor Appl Clim 87:85–102. https://doi.org/10.1007/s00704-005-0224-2

Shrestha M, Acharya S, Shrestha PK (2017) Bias correction of climate models for hydrological modelling–are simple methods still useful? Meteorol Appl 24(3):531–539. https://doi.org/10.1002/met1655

Spinoni J, Vogt JV, Naumann G, Barbosa P, Dosio A (2018) Will drought events become more frequent and severe in Europe? Int J Clim 38(4):1718–1736. https://doi.org/10.1002/joc5291

Spinoni J, Naumann G, Vogt JV, Barbosa P (2015) The biggest drought events in Europe from 1950 to 2012. J Hydrol Reg Stud 3:509–524. https://doi.org/10.1016/j.ejrh.2015.01.001

Stagge JH, Tallaksen LM, Gudmundsson L, Van Loon AF, Stahl K (2015) Candidate distributions for climatological drought indices (SPI and SPEI). Int Climatol 35(13):4027–4040. https://doi.org/10.1002/joc.4267

Taylor KE, Stouffer RJ, Meehl GA (2012) An overview of CMIP5 and the experiment design. Bull Amer Meteor Soc 93(4):485–498. https://doi.org/10.1175/BAMS-D-11-000941

Terzago S, Cremonini R, Cassardo C, Fratianni S (2012) Analysis of snow precipitation during the period 2000–09 and evaluation of a snow cover algorithm in Sw Italian Alps. Geogr Fis Din Quat 35:91–99. https://doi.org/10.4461/gfdq201235

Terzi S, Sušnik J, Schneiderbauer S, Torresan S, Critto A (2021) Stochastic system dynamics modelling for climate change water scarcity assessment of a reservoir in the Italian Alps. Nat Hazards Earth Syst Sci 21(11):3519–3537. https://doi.org/10.5194/nhess-21-3519-2021

Teuling AJ (2018) A hot future for European droughts. Nat Clim Change 8(5):364–365. https://doi.org/10.1038/s41558-018-0154-5

Teutschbein C, Seibert J (2012) Bias correction of regional climate model simulations for hydrological climate-change impact studies: review and evaluation of different methods. J Hydrol 456:12–29. https://doi.org/10.1016/jjhydrol201205052

Tirivarombo S, Osupile D, Eliasson P (2018) Drought monitoring and analysis: standardised precipitation evapotranspiration index (SPEI) and standardised precipitation index (SPI). Phys Chem Earth 106:1–10. https://doi.org/10.1016/jpce201807001

Toreti A, Desiato F (2008) Temperature trend over Italy from 1961 to 2004. Theor Appl Climatol 91(1–4):51–58. https://doi.org/10.1007/s00704-006-0289-6

Trenberth KE, Dai A, van der Schrier G, Jones PD, Barichivich J, Briffa KR, Sheffield J (2013) Global warming and changes in drought. Nat Clim Change 4(1):17–22. https://doi.org/10.1038/nclimate2067

Turco M, Rosa-Cánovas JJ, Bedia J, Jerez S, Montávez JP, Llasat MC, Provenzale A (2018) Exacerbated fires in Mediterranean Europe due to anthropogenic warming projected with non-stationary climate-fire models. Nat Sci Rep 9(1):1–9. https://doi.org/10.1038/s41467-018-06358-z

Vallorani R, Bartolini G, Betti G, Crisci A, Gozzini B, Grifoni D, Maracchi G (2018) Circulation type classifications for temperature and precipitation stratification in Italy. Int J Climatol 38(2):915–931. https://doi.org/10.1002/joc5219

Vicente-Serrano SM, Tomas-Burguera M, Beguería S, Reig F, Latorre B, Pena-Gallardo M, González-Hidalgo JC (2017) A high resolution dataset of drought indices for Spain. Data 2(3):22. https://doi.org/10.3390/data2030022

Vicente-Serrano SM, Azorin-Molina C, Sanchez-Lorenzo A, Revuelto J, Lopez-Moreno JI, Gonzalez-Hidalgo JC, Espejo F (2014) Reference evapotranspiration variability and trends in Spain, 1961–2011. Glob Planet Change 121:26–40. https://doi.org/10.1016/jgloplacha201406005

Vicente-Serrano SM, Beguería S, López-Moreno JI (2010) A multiscalar drought index sensitive to global warming: the standardized precipitation evapotranspiration index. J Clim 23(7):1696–1718. https://doi.org/10.1175/2009JCLI29091

Zimmermann NE, Gebetsroither E, Zuger J, et al (2013) Future Climate of the European Alps. In: Cerbu G (ed.), Management strategies to adapt Alpine space forests to climate change risks. In Tech, Rijeka, Croatia. pp 27–36. https://doi.org/10.5772/56278